PREDICTION OF THE ACOUSTIC PERFORMANCE OF SMALL POROELASTIC FOAM FILLED MUFFLERS: A CASE STUDY

P. W. Jones
School of Mechanical and Manufacturing Engineering, The University of New South Wales, Sydney NSW 2052, Australia

The acoustic performance of small, irregularly shaped mufflers in continuous positive airway pressure (CPAP) devices is often enhanced by the inclusion of dissipative materials. In this study, the acoustic properties of two polyurethane foams were determined using a two-cavity method. Acoustic models of two CPAP device muffler designs incorporating a foam insert have been developed using a commercial finite element analysis software package. Experimental results for the mufflers have been obtained using the two-microphone acoustic pulse method. Results of the transmission loss of the muffler designs obtained from the finite element models are presented and validation of the computational results is discussed.

INTRODUCTION

Continuous positive airway pressure (CPAP) devices generate air flow using a high speed fan and noise from this device is controlled using mufflers situated in the flow path at the fan inlet and the flow generator outlet. While the most significant noise levels are present at frequencies below 4 kHz, the use of dissipative materials is often utilised in order to extend the attenuated frequency range up to 10 kHz.

Foundation work on the theoretical approach to describe sound propagation in porous materials was laid by Zwikker and Kosten [1] who introduced the concept of effective density and bulk modulus. Biot [2, 3] introduced frame elasticity, where the skeleton of the material is not rigid and is capable of transmitting sound waves. A key element of this work was identification of the existence of three types of sound wave for continuous materials: two compression waves and one shear wave. Morse and Ingard [4] developed generic acoustic models for rigid and limp porous materials. Lambert studied low and medium flow resistance foams [5] and this work was extended by Allard *et al*. [6] to high flow resistance foams. Allard and Champoux [7] used the general frequency dependence of the viscous forces in porous materials proposed by Johnson *et al*. [8] to produce expressions incorporating five macroscopic properties of the porous material. Delany and Bazley [9] showed that measured values of characteristic impedance and propagation coefficient for a range of fibrous materials, normalised as a function of frequency divided by flow resistance, could be presented as simple power law functions. Miki [10] found that the Delany-Bazley model produced an unphysical prediction at low frequencies and amended the original equation regression coefficients. Further work was done by Bies and Hansen [11] and Mechel [12] to correct and extend the Delany-Bazley method beyond the bounds recommended by the original authors. Attenborough [13] observed that the normalising parameter used by Delany and Bazley appeared in the theoretical expressions for any pore shape and concluded that empirical relationships of the form proposed by Delany and Bazley should be valid for non-fibrous porous materials. He did however also note that "frame elasticity will be an additional complication" and that the coefficients in the Delany-Bazley model would be unique to each type of porous material. Dunn and Davern [14] followed the same approach used by Delany and Bazley and derived new regression coefficients which applied the power law functions to polyurethane foams. Work by Wu [15] and Ling [16] has resulted in the derivation of further sets of regression coefficients for medium and high flow resistivity foams. Komatsu [17] showed that the coefficients used in the Delany-Bazley model were strongly dependent on the airflow resistivity and introduced a common logarithm term in place of the original non-dimensional normalising parameter.

This study builds on previous work by the authors on acoustic finite element (FE) modelling of reactive muffler designs [18]. The acoustic characteristics of two polyurethane foams were obtained experimentally and the corresponding properties incorporated into FE models of a production CPAP muffler and a prototype integrated chamber design. Results of the transmission loss of the foam-filled mufflers obtained from the FE models are presented. The transmission loss of each of the mufflers was measured using a two-microphone acoustic pulse method which was based on the procedure developed by Seybert and Ross [19]. For the two muffler designs, experimental results for an empty muffler and the muffler containing an insert manufactured from each foam type are compared with results obtained computationally.

MUFFLER DESIGNS

Two muffler designs which were originally presented in the previous paper by the authors [18] were selected for further analysis. The first design shown in Figure 1 is that of a production CPAP device muffler which, while geometrically complex, consists of a single chamber having coaxial inlet and outlet ports located at one end of the chamber. A foam

insert, shown by the grey shaded area in Figure 2, occupies the majority of the chamber volume. It is important to note that this insert does not intrude into the direct path between the inlet and outlet ports. The second design shown in Figure 3 consists of two integrated chambers and presents a complex path between the inlet and outlet ports. If air is flowing through the device it would be deflected around a vertical internal baffle before passing through a narrow slot into the final chamber. A foam insert completely fills the volume of the first chamber and sound waves entering from the inlet port must pass through the foam prior to reaching the outlet port.

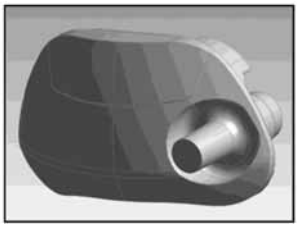

Figure 1a: CPAP muffler air volume

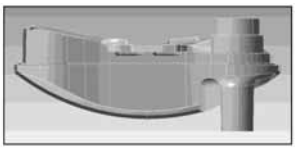

Figure 1b: Muffler cross-section

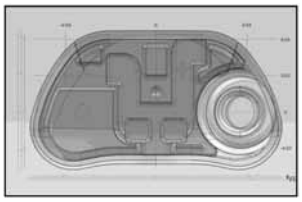

Figure 2a: CPAP muffler foam insert (front)

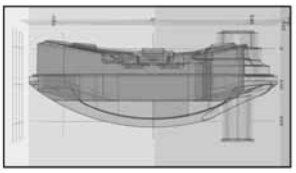

Figure 2b: CPAP muffler foam insert (top)

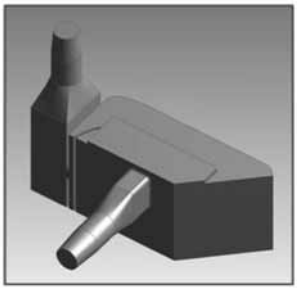

Figure 3a: Integrated muffler air volume

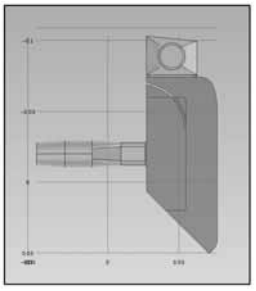

Figure 3b: Muffler foam insert

Two different polyurethane foam materials were selected for comparison. The first foam (light grey) has an apparent density of 34 kg/m^3 and is a material currently being used in CPAP device mufflers. The second foam (dark grey) has an apparent density of 23 kg/m^3 and is more likely to be used in protective packaging. The latter was chosen for inclusion in the assessment as it was anticipated that the acoustic properties would be sufficiently dissimilar to the first to provide an instructive comparison.

FOAM MODELLING METHOD

Characteristic impedance ($Z_{c,f}$) and propagation coefficient (γ_f) of porous materials can be presented as simple power-law functions by [9, 11]:

$$Z_{c,f} = R + jX \;, \quad Z_{c,f} = \rho_a c_a \left[1 + C_1\left(\frac{\rho_a f}{r_f}\right)^{C_2} - j * C_3\left(\frac{\rho_a f}{r_f}\right)^{C_4}\right] \qquad (1)$$

$$\gamma_f = \propto + j\beta \;, \quad \gamma_f = (\omega / c_a)\left[C_5\left(\frac{\rho_a f}{r_f}\right)^{C_6} + j\left(1 + C_7\left(\frac{\rho_a f}{r_f}\right)^{C_8}\right)\right] \qquad (2)$$

where ρ_a and c_a are respectively the density and speed of sound in air, f is the frequency and r_f is the airflow resistivity. Delany and Bazley obtained values for the coefficients C_1 to C_8 using a range of fibrous absorbent materials [9]. Several authors have noted that predictions made using Delany and Bazley's original coefficients are not especially accurate when applied to poroelastic materials and have obtained different sets of coefficients [10, 14-16]. In this work, the characteristic impedance, propagation coefficient and airflow resistivity of the two foams materials were measured experimentally. The methodology described by Delany and Bazley was then applied to derive the unknown coefficients C_1 to C_8 for these particular foams. Once the coefficients have been determined and substituted back into Eqs. (1) and (2), the resulting equations are then readily incorporated directly into the finite element model. Further insight into the acoustic performance of the foams may be gained by re-stating Eqs. (1) and (2) in terms of an equivalent fluid having a complex speed of sound (c_f) and complex mean density (ρ_f) by [19]:

$$c_f = j\frac{\omega}{\gamma_f} \;, \quad c_f = \left[\frac{\omega\beta}{(\alpha^2 + \beta^2)}\right] + j\left[\frac{\omega\alpha}{(\alpha^2 + \beta^2)}\right] \qquad (3)$$

$$\rho_f = -j\frac{Z_{c,f}\gamma_f}{\omega} \;, \quad \rho_f = \left[\frac{(R\beta + X\alpha)}{\omega}\right] + j\left[\frac{(X\beta - R\alpha)}{\omega}\right] \qquad (4)$$

EXPERIMENTAL METHODS

Experimental methods used to obtain the characteristic impedance, propagation constant and flow resistivity of the foams are presented in what follows. Further experiments were then conducted to measure the transmission loss of the mufflers using the two-microphone acoustic pulse method, which has been described previously [18].

Characteristic impedance and propagation constant

The characteristic impedance and propagation constant of porous materials can be measured by applying the transfer function method to a two-cavity approach [20]. A sample of homogeneous porous material was positioned within a Brüel & Kjær Type 4206 impedance tube and against the front face of a moveable plunger. The plunger was then withdrawn away from the sample, producing an air cavity with a known depth L between the rear face of the sample and the plunger (Fig. 4). A random signal was fed to the loudspeaker of the impedance

tube and the normal surface acoustic impedance of the sample was measured in accordance with ISO 10534 [21]. The transfer function H_{12} from microphone position 1 to position 2, defined by the complex ratio p_2/p_1, was measured using a two channel Fast Fourier transform. The surface acoustic impedance Z_0 is then obtained by [22]:

$$Z_0 = jZ_{c,a}\left\{\frac{H_{12}\sin[k(Lx+Dx)] - \sin(kLx)}{\cos(kLx) - H_{12}\cos[k(Lx+Dx)]}\right\} \quad (5)$$

where k is the wave number and $Z_{c,a}(=\rho_a c_a)$ is the characteristic impedance of air.

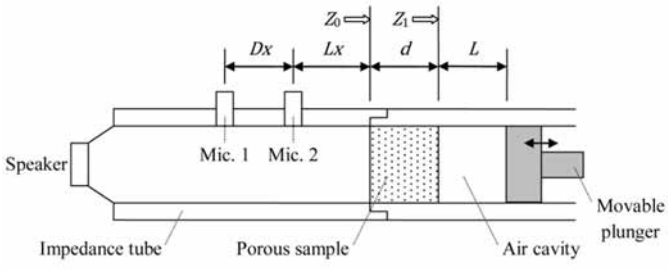

Figure 4: Schematic diagram of the impedance tube configuration

The impedance tube plunger was withdrawn a further distance and the measurement procedure was repeated at depth L' to obtain Z_0'. The theoretical impedance of closed tubes with depths L and L' is given by [20]:

$$Z_1 = -jZ_a\cot(kL), \quad Z_1' = -jZ_a\cot(kL') \quad (6,7)$$

The characteristic impedance and propagation constant of the material can then be calculated by [20]:

$$Z_{c,f} = \pm\sqrt{\frac{Z_0Z_0'(Z_1 - Z_1') - Z_1Z_1'(Z_0 - Z_0')}{(Z_1 - Z_1') - (Z_0 - Z_0')}} \quad (8)$$

$$\gamma_f = \left(\frac{1}{2d}\right)\ln\left[\left(\frac{Z_o + Z_{c,f}}{Z_o - Z_{c,f}}\right)\left(\frac{Z_1 - Z_{c,f}}{Z_1 + Z_{c,f}}\right)\right] \quad (9)$$

where the sign in Eq. (8) is selected so that the real part of $Z_{c,f}$ is positive.

Airflow resistivity

The airflow resistivity of a homogeneous material is given by $r_f = \Delta P / du$, where ΔP is the static pressure drop across the material, d is the unit thickness and u is the linear velocity of air passing through it [23]. Measurements were performed according to the direct airflow method described in ISO 9053 [23]. A unidirectional airflow was passed through cylindrical samples having 25mm thickness and 100mm diameter (see Fig. 5) and the resulting pressure drop between the two free faces of the sample was measured.

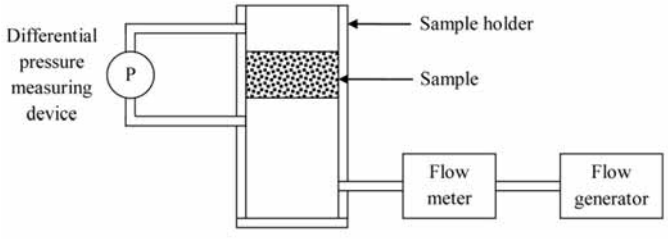

Figure 5: Schematic diagram of the airflow resistivity experimental set-up

FINITE ELEMENT MODELS

Acoustic finite element models of each of the muffler designs were developed using the commercially available finite element analysis package COMSOL (version 4.0). The muffler models were meshed using Lagrange-quadratic elements with controls applied to produce a mesh having at least 6 elements per acoustic wavelength at the upper bound of the frequency range being analysed (limiting case). A harmonic pressure of 1 Pa was specified at the inlet and a radiation condition applied at inlet and outlet. The air was assumed to be non-flowing and inviscid and acoustic damping was not applied at the fluid-structure interface. The foam inserts were modelled using the Delany-Bazley formulation described earlier and having parameters that were obtained experimentally for each of the foam types. Transmission loss is calculated directly in COMSOL using the acoustic power at the inlet and outlet ports of the muffler.

RESULTS AND DISCUSSION

The results are presented in three sub-sections corresponding to the foam airflow resistivity measurements, foam acoustic property measurements (characteristic impedance and propagation constant) and the muffler transmission loss measurements, respectively.

Foam airflow resistivity

Airflow resistivity for each foam type was measured according to the direct airflow method described in ISO 9053. Data was also recorded at linear airflow velocities greater than the 4 mm/s upper limit recommended by the Standard to ascertain the effect of turbulent flow on the apparent airflow resistivity for the foams being studied. The values for airflow resistivity calculated using data within the laminar range are presented in Table 1 and it can be seen that the measured airflow resistivity of the two foam types is significantly different. This finding is consistent with the observed difference in surface pore sizes and spacing.

Table 1: Foam airflow resistivity

Foam	Description	Flow resistivity (Rayls/m)	95% confidence interval
A	Acoustic (light grey)	8,445	182
B	Non-acoustic (dark grey)	2,652	36

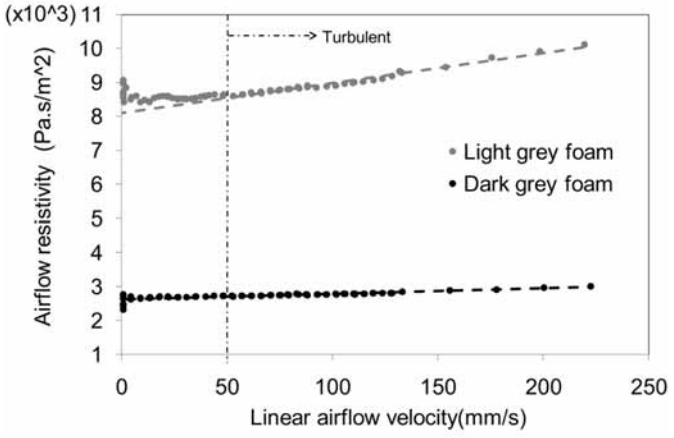

Figure 6: Airflow resistivity of dark and light grey foams

Figure 6 shows that the apparent airflow resistivity for the light grey foam increases as the linear airflow is increased beyond the laminar region, while the apparent airflow resistivity of the dark grey foam remains largely unaffected. This difference in observed behaviour is significant as the Delany-Bazley method uses a single value for flow resistivity to characterise the porous material.

Foam acoustic properties

The normal surface impedance for each foam type was measured and calculated using the test method described in ISO 10534. Measurements were obtained at four cavity depths corresponding to 25mm, 50mm, 75mm, and 100mm, using samples of 25mm thickness. The characteristic impedance and propagation constant were calculated for each of the cavity combinations 25mm/50mm, 50mm/75mm and 75mm/100mm using Eqs. (8) and (9) and the results for the three combinations were averaged. Equations (1) and (2) can be re-stated as:

$$\log_{10}\frac{R}{\rho_a\, c_a} - 1 = C_2\log_{10}\left(\frac{\rho_a\, f}{r_f}\right) + \log_{10}(C_1) \tag{10}$$

$$\log_{10}\left(\frac{-X}{\rho_a\, c_a}\right) = C_4\log_{10}\left(\frac{\rho_a\, f}{r_f}\right) + \log_{10}(C_3) \tag{11}$$

$$\log_{10}\left(\frac{\alpha c_a}{\omega}\right) = C_6\log_{10}\left(\frac{\rho_a\, f}{r_f}\right) + \log_{10}(C_5) \tag{12}$$

$$\log_{10}\left(\frac{\beta c_a}{\omega} - 1\right) = C_8\log_{10}\left(\frac{\rho_a\, f}{r_f}\right) + \log_{10}(C_7) \tag{13}$$

As Eqs. (10) to (13) are of the form $y = mx + b$, it is possible to obtain the equation coefficients by fitting linear trend lines through the experimental data. The coefficients that were obtained are presented in Table 2 alongside Delany and Bazley's original coefficients. It can be seen that the coefficients for each of the two foam types are significantly different from each other and also from the original Delany-Bazley coefficients, with the exception of the attenuation constant α which shows reasonable agreement. These differences support previous findings that predictions made using the original Delany-Bazley coefficients are not especially accurate when applied to poroelastic materials [10, 14-16] and that the coefficients would be unique to each type of porous material [13]. However it is worth noting that the propagation constant of both foam types correlate well with the flow resistivity, producing correlation coefficients between 0.96 and 0.99. The characteristic impedance of the light grey foam also correlates well, producing correlation coefficients between 0.88 and 0.92. These observations are consistent with the findings of Wu [15] who reported correlation coefficients between 0.85 and 0.99 for porous plastic open-celled foams. While the correlation coefficients for the characteristic impedance of the dark grey foam are less encouraging (0.58 and 0.72), examination of the characteristic impedance curves shows significant departure from linear behaviour at frequencies greater than 1,600 Hz. This suggests that the observed behaviour might be attributed to sample preparation as this frequency coincides with the transition between measurements obtained in the 100mm diameter impedance tube and those obtained in the 29mm diameter impedance tube.

The Delany-Bazley relationships are only considered to be valid over the range $0.012 \leq (\rho_a f / r_f) \leq 1.2$ [11]. Assuming an air density of 1.18 kg/m^3, the valid frequency range for the dark grey foam is 25 Hz to 2,690 Hz, while for the light grey foam it is 85 Hz to 8,500 Hz.

Equations (3) and (4) were used to obtain the complex speed of sound and complex density of the two foam materials based on the coefficients in Table 2. The results for the speed of sound and density of the light grey foam are shown in Figs. 7 and 8, respectively. The Delany-Bazley model shows excellent agreement with the experimental data. This is not unexpected as the model coefficients were derived using the same set of experimental data and the correlation coefficients were good. The results for the dark grey foam show a comparable agreement between the model and the experimental data, with only slight deviation noted between the model and the data at frequencies below 250 Hz. This deviation is attributed to the lower correlation coefficients associated with the impedance equation.

Table 2: Delany-Bazley equation coefficients

Parameters		Dark grey foam		Light grey foam		Delany & Bazley
		Coefficient	R^2	Coefficient	R^2	Coefficient
R (Z_c)	C_1	0.2051	0.58	0.2824	0.92	0.0571
	C_2	-0.2249		-0.3659		-0.7540
X (Z_c)	C_3	0.1175	0.72	0.0980	0.88	0.0870
	C_4	-0.4851		-0.6144		-0.7320
α (γ)	C_5	0.2039	0.98	0.1692	0.99	0.1890
	C_6	-0.5416		-0.5728		-0.5950
β (γ)	C_7	0.2688	0.96	0.2561	0.97	0.0978
	C_8	-0.3111		-0.4657		-0.7000

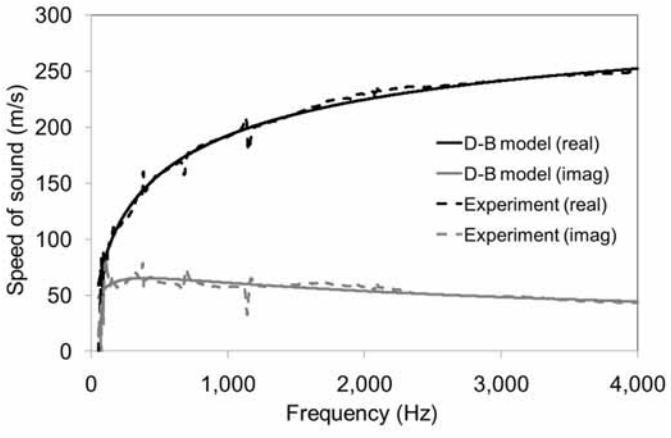

Figure 7: Equivalent fluid speed of sound of light grey foam

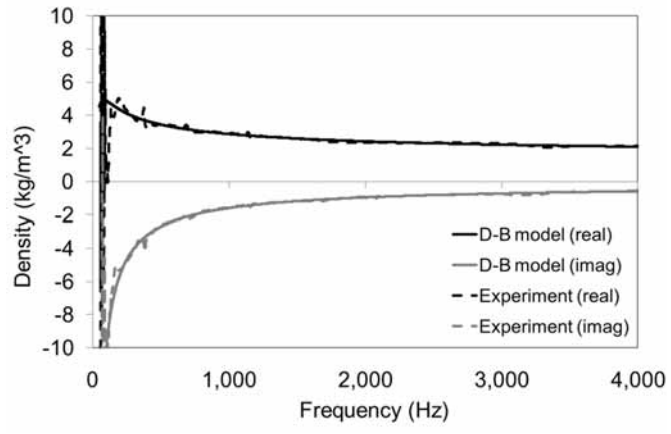

Figure 8: Equivalent fluid density of light grey foam

Muffler transmission loss

Figure 9 contains the transmission loss obtained experimentally for the CPAP device muffler, with and without a foam insert present, and the transmission loss predicted by the COMSOL finite element model. The FE results show good agreement with the experimental results over the frequency range assessed. The inclusion of the foam insert results in slight degradation of performance at the lower frequencies, especially about the peak centred at 800 Hz, but also results in a transmission loss of at least 10 dB over a broadband frequency range above that peak. Figure 10 compares the transmission loss obtained computationally and experimentally for the CPAP device muffler using the light and dark grey foams. The results show that the foam inserts have a very similar impact on the acoustic performance of this muffler design despite a difference in apparent density of approximately 50%.

Figure 11 contains the transmission loss predicted by the finite element model for the integrated chamber muffler both with and without the first chamber filled with foam. The results show that the presence of foam has little effect on the acoustic performance of the muffler below 500 Hz but contributes significantly to increased transmission loss at higher frequencies. In contrast to the observations made in respect to the CPAP device muffler, the results show that the two foam materials make differing contributions to the acoustic performance of this muffler design.

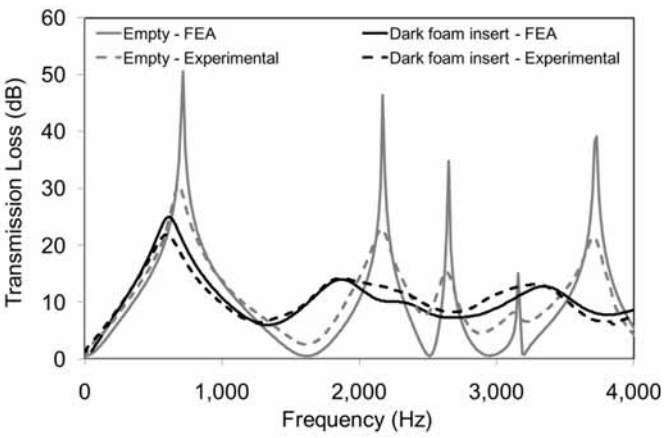

Figure 9: Transmission loss for the CPAP device muffler with and without dark foam insert, comparing computational results (solid lines) and experimental results (dashed lines)

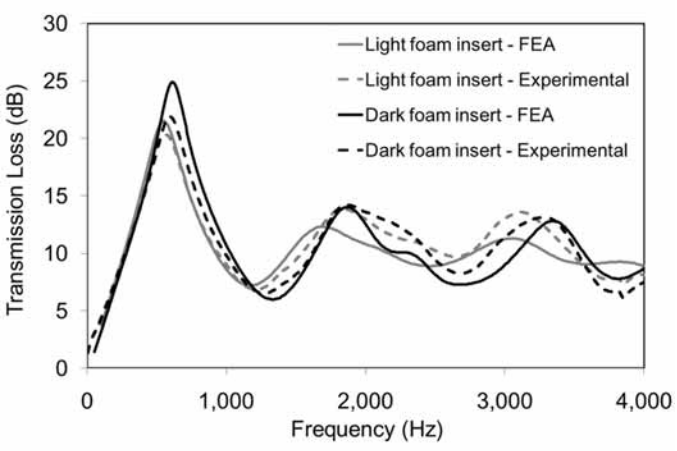

Figure 10: Transmission loss for the CPAP device muffler with foam inserts, comparing computational results (solid lines) and experimental results (dashed lines)

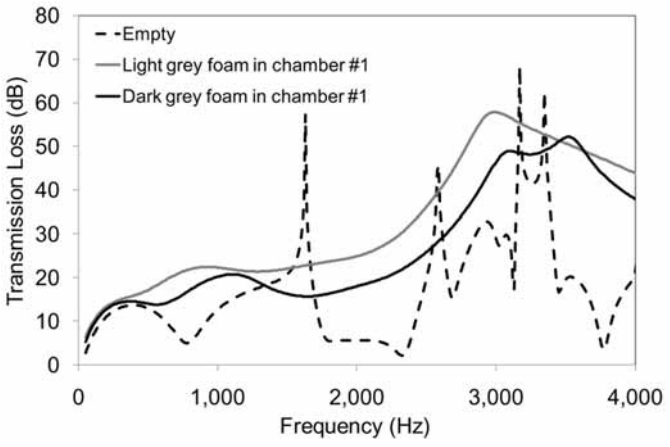

Figure 11: Transmission loss results obtained computationally for the integrated muffler without foam (dashed line) and with the first chamber foam filled (solid lines)

This observation is attributed to the muffler designs and location of the foam inserts. In the case of the integrated chamber design, sound waves travelling between the inlet and outlet ports are required to pass through the foam while in the CPAP device design, they only graze the surface of the foam insert. The greater contribution made by the light grey foam is consistent with the higher apparent density and flow resistivity when compared to the dark grey foam.

CONCLUSIONS

The characteristic impedance and propagation constant of two polyurethane foams have been determined experimentally using a two-cavity impedance tube method. Airflow resistivity of the two foams has been determined experimentally using the direct airflow method described in ISO 9053. Acoustic models of a production CPAP device muffler and an integrated chamber muffler design, both incorporating poroelastic foam inserts, have been developed using a commercial finite element analysis software package. Transmission loss results for the mufflers have been experimentally obtained using the two-microphone acoustic pulse method.

The magnitudes of the airflow resistivity measured for each of the two foam types are significantly different and they also exhibit differing sensitivity to linear airflow variations. The Delany-Bazley equation coefficients calculated for each of the two foam types differ from the original Delany-Bazley coefficients and also from each other. As the original Delany-Bazley model assumes a single value for flow resistivity to characterise the porous material and applies a fixed set of equation coefficients to model all porous materials, use of the original Delany-Bazley model to represent these foams will lead to inaccurate predictions.

Transmission loss results for the two muffler designs with and without the foam inserts were presented. The transmission loss results obtained computationally incorporated the derived Delany-Bazley coefficients. Good agreement between the numerical and experimental results was obtained for both muffler designs across the entire considered frequency range. The foam inserts make little impact on the acoustic performance of either muffler design below 500 Hz and results in slight degradation of performance about the peak centred at 800 Hz in the case of the CPAP device muffler. The inserts make a positive contribution to the transmission loss of both muffler designs at higher frequencies. The light grey foam makes a greater contribution than the dark grey foam which is consistent with its higher apparent density and flow resistivity. The effect of the foam inserts on the muffler acoustic performance is more significant in the integrated chamber design, which is attributed to the sound waves passing through approximately 20cm of foam between the inlet and the outlet ports whereas in the CPAP device design the sound waves only graze the surface of the foam insert.

By characterising foam as an equivalent fluid using straight-forward airflow resistivity and impedance tube measurements, it has been shown that accurate predictions of the acoustic performance of foam inserts in small mufflers can be achieved using finite element modelling.

ACKNOWLEDGEMENTS

Financial assistance for this work was provided as part of an ARC Linkage Project jointly funded by the Australian Research Council and ResMed.

REFERENCES

[1] C. Zwikker and C.W. Kosten, *Sound Absorbing Materials*, Elsevier, New York (1949)

[2] M.A. Biot, "Theory of propagation of elastic wave in a fluid saturated porous solid", *J. Acoust. Soc. Am.*, **28**, 168-78 (1956)

[3] M.A. Biot, "Mechanics of deformation and acoustic propagation in porous media", *J. Appl. Phys.*, **33**, 1482-1498

[4] P.M. Morse and K.U. Ingard, *Theoretical Acoustics*, McGraw-Hill, New York (1968), pp. 241-56

[5] R.F. Lambert, "Propagation of sound in highly porous open-cell foams", *J. Acoust. Soc. Am.*, **73**, 1131-8 (1982)

[6] J.F. Allard, A. Aknine, and C. Depollier, "Acoustical properties of partially reticulated foams with high and medium flow resistance", *J. Acoust. Soc. Am.* , **72**, 1734-40 (1986)

[7] J.F. Allard and Y. Champoux, "New empirical equations for sound propagation in rigid frame fibrous materials", *J. Acoust. Soc. Am.*, **91** (6), 3346-53 (1992)

[8] D.L. Johnson, J. Koplik and R. Dashen, "Theory of dynamic permeability and tortuosity in fluid-saturated porous media", *J. Fluid Mech.*, **176**, 379-402 (1987)

[9] M.E. Delany and E.N. Bazley, "Acoustical properties of fibrous absorbent materials", *Appl. Acoust.*, **3**, 105-116 (1970)

[10] Y. Miki, "Acoustical properties of porous materials – Modifications of Delany-Bazley models", *J. Acoust. Soc. Jpn,* **11**(1), 19-28 (1990)

[11] D.A. Bies and C.H. Hansen, "Flow resistance information for acoustical design", *Appl. Acoust.*, **13**, 357-391 (1980)

[12] F.P. Mechel, "Chapter 8 - Sound-absorbing materials and sound absorbers" in *Noise and Vibration Control Engineering*, ed. Beranek, L.L. and Vér, I.L., John Wiley and Sons, New York (1992)

[13] K. Attenborough, "Acoustical characteristics of porous materials", *Phys. Rep.*, **82**(3), 179-227 (1982)

[14] I.P. Dunn and W.A. Davern, "Calculation of acoustic impedance of multi-layer absorbers", *Appl. Acoust.*, **19**, 321-334 (1986)

[15] Q. Wu, "Empirical Relations between Acoustical Properties and Flow Resistivity of Porous Plastic Open-Cell Foam", *Appl. Acoust.*, **25**, 141-148 (1988)

[16] M.K. Ling, "Technical Note – Impedance of polyurethane foams", *Appl. Acoust.*, **34**, 221-224 (1991)

[17] T. Komatsu, "Improvement of the Delany-Bazley and Miki models for fibrous sound-absorbing materials", *Acoust. Sci. & Tech.*, **29**(2), 121-129 (2008)

[18] P.W. Jones and N.J. Kessissoglou, "A numerical and experimental study of the transmission loss of mufflers used in respiratory medical devices", *Acoust. Aust.*, **38**(1), 13-19 (2010)

[19] O.Z. Mehdizadeh and M. Paraschivoiu, "A three dimensional finite element approach for predicting the transmission loss in mufflers and silencers with no mean flow", *Appl. Acoust.*, **66**, 902-918 (2005)

[20] H. Utsuno, T. Tanaka, T. Fujikawa and A.F. Seybert, "Transfer function method for measuring characteristic impedance and propagation constant of porous materials", *J. Acoust. Soc. Am.*, **86**(2), 637-643 (1989)

[21] ISO 10534-2:1998: Acoustics – *Determination of sound absorption coefficient and impedance in impedance tubes* – Part 2: *Transfer-function method*, International Organisation for Standardization, Switzerland (1998)
[22] M.L. Munjal and A.G. Doige, "The two-microphone method incorporating the effects of mean flow and acoustic damping", *J. Sound Vib.*, **137**(1), 135-138 (1990)
[23] ISO 9053:1991: *Acoustics – Materials for acoustical applications – Determination of airflow resistance*, International Organisation for Standardization, Switzerland (1991)

26 – 31 August 2010, Sydney and Katoomba
ISMA 2010 International Symposium on Musical Acoustics
http://isma2010.phys.unsw.edu.au/

29 – 31 August 2010, Melbourne
ISRA 2010 International Symposium on Room Acoustics
http://www.isra2010.org/

29 – 31 August 2010, Auckland, New Zealand
ISSA 2010 International Symposium on Sustainability in Acoustics
http://issa.acoustics.ac.nz